

This is the final draft of the contribution published as:

Makkonen, J., Jussila, J., Panteleit, J., **Keller, N.S.**, Schrimpf, A., Theissinger, K., Kortet, R., Martín-Torrijos, L., Sandoval-Sierra, J.V., Diéguez-Uribeondo, J., Kokko, H. (2018):
MtDNA allows the sensitive detection and haplotyping of the crayfish plague disease agent
Aphanomyces astaci showing clues about its origin and migration
Parasitology **145** (9), 1210 - 1218

The publisher's version is available at:

<http://dx.doi.org/10.1017/S0031182018000227>

MtDNA allows the sensitive detection and haplotyping of the crayfish plague disease agent *Aphanomyces astaci* showing clues about its origin and migration

Jenny Makkonen¹*, Japo Jussila¹, Jörn Panteleit²), Nina Sophie Keller^{2,3}), Anne Schrimpf²), Kathrin Theissinger²), Raine Kortet⁴), Laura Martín-Torrijos⁵), Jose Vladimir Sandoval-Sierra⁵), Javier Diéguez-Uribeondo⁵), and Harri Kokko¹)

¹ Department of Environmental and Biological Sciences, University of Eastern Finland, P.O. Box 1627, FI-70211, Kuopio, Finland

² University of Koblenz-Landau, Institute for Environmental Sciences, Fortstrasse 7, D-76829 Landau, Germany

³ Helmholtz-Centre for Environmental Research (UfZ), Department of Isotope Biogeochemistry, Permoserstrasse 15, D-04318 Leipzig, Germany

⁴ Department of Environmental and Biological Sciences, University of Eastern Finland, P.O. Box 111, FI-80101, Joensuu, Finland

⁵ Department of Mycology, Real Jardín Botánico CSIC, Plaza de Murillo 2, ES-28014 Madrid, Spain

Corresponding author: jenny.makkonen@uef.fi, tel. +358 50 430 2042

Running head: *Aphanomyces astaci* haplotyping

SUMMARY

The oomycete *Aphanomyces astaci*, the causative agent of crayfish plague, is listed as one of the 100 worst invasive species in the world, destroying the native crayfish populations throughout Eurasia. The aim of this study was to examine the potential of selected mitochondrial (mt) genes to track the diversity of the crayfish plague pathogen *A. astaci*. Two sets of primers were developed to amplify the mtDNA of ribosomal rnnS and rnnL subunits. We confirmed two main lineages, with four different haplogroups and five haplotypes among 27 studied *A. astaci* strains. The haplogroups detected were 1) the A-haplogroup with the a-haplotype strains originating from *Orconectes* sp., *Pacifastacus leniusculus*, and *Astacus astacus* 2) the B-haplogroup with the b-haplotype strains originating from the *Pacifastacus leniusculus*, 3) the D-haplogroup with the d1 and d2-haplotypes strains originating from *Procambarus clarkii*, and 4) the E-haplogroup with the e-haplotype strains originating from the *Orconectes limosus*. The described markers are stable and reliable and the results are easily repeatable in different laboratories. The present method has high applicability as it allows the detection and characterization of the *A. astaci* haplotype in acute disease outbreaks in the wild, directly from the infected crayfish tissue samples.

Keywords: invasive species, oomycete, crayfish disease, single nucleotide polymorphism, ribosomal rnnS and rnnL subunits

INTRODUCTION

The crayfish plague, caused by *Aphanomyces astaci* (Schikora), is the most devastating crayfish disease known to date (Cerenius *et al.* 2009; Jussila *et al.* 2015). *Aphanomyces astaci* is listed among the 100 worst invasive species in the world by the Global Invasive Species Specialist Group of the International Union for Conservation of Nature (IUCN; Lowe *et al.* 2004), being the main reason for the reducing numbers of the native crayfish throughout Europe (Souty-Grosset *et al.* 2006). All the five European crayfish species, *i.e.*, noble crayfish (*Astacus astacus*), stone crayfish (*Austropotamobius torrentium*), white-clawed crayfish (*Austropotamobius pallipes*), narrow-clawed crayfish (*Astacus leptodactylus*), and thick-clawed crayfish (*Astacus pachypus*), are susceptible to the disease, with catastrophic epidemics possible, and the three first mentioned species are listed in the IUCN Red list as vulnerable, with a decreasing population trend (IUCN, 2012).

During the past decades, phylogenetic studies on different *A. astaci* strains have been done to clarify the relationships within this species and the North American hosts that carry them. The Random amplification of polymorphic DNA–polymerase chain reaction (RAPD-PCR) techniques firstly revealed certain genetic diversity in *A. astaci* (Huang *et al.* 1994; Diéguez-Uribeondo *et al.* 1995; Rezinciuc *et al.* 2014). Thus, five genetic groups of *A. astaci*, named A, B, C, D, and E, have been identified in Europe by using RAPD-PCR (Huang *et al.* 1994; Diéguez-Uribeondo *et al.* 1995; Kozubíková *et al.* 2011). The RAPD-PCR group A (As) includes the strain of reference L1, which was isolated from native European crayfish *A. astacus*, and also a number of strains that seem to be related to the first invasion of *A. astaci* with an unknown host species in the 19th century. The RAPD-PCR group B (PsI) includes the strain of reference Pl, which was isolated from the North American crayfish species, *Pacifastacus leniusculus*, as well as other strains isolated from outbreaks in native European species and other *P. leniusculus* crayfish. The RAPD-PCR group C (PsII) is comprised of a single strain named Kv, isolated from an outbreak on signal crayfish in Kvarntorp (Sweden) that originated from Lake Pitt (Canada) (Huang *et al.* 1994). This group has not been detected since then (Söderhäll and Cerenius, 1999). The RAPD-PCR group D (Pc) includes the reference strain Pc and was first isolated from the red swamp crayfish (*Procambarus clarkii*) in Spain (Diéguez-Uribeondo and Söderhäll, 1993; Diéguez-Uribeondo *et al.* 1995) and a number of strains, *e.g.*, APO3 and Málaga5, isolated from outbreaks in native crayfish *A. pallipes* (Rezinciuc *et al.* 2014). Finally, the RAPD-PCR group E (Or) comprises a reference strain Evira4805 isolated from the spiny-cheek crayfish (*Orconectes limosus*) naturalized in Europe

(Kozubíková *et al.* 2011) and a few strains isolated from outbreaks in native crayfish *A. astacus*, *e.g.* Li10, after that (Kozubíková-Balcarová *et al.* 2013).

Later, studies based on Internal transcribed spacer (ITS)-regions indicated that *A. astaci* strains were genetically very similar since their intraspecific variation measured is close to zero (Diéguez-Uribeondo *et al.* 2009; Makkonen *et al.* 2011). It was postulated that this was a result of the clonal propagation via zoospores (Huang *et al.* 1994; Diéguez-Uribeondo *et al.* 2009; Rezinciuc *et al.* 2015). Additional studies exploring the *A. astaci* diversity in Europe were conducted on nuclear chitinase gene (Makkonen *et al.* 2012a), amplified fragment length polymorphisms (AFLP; Rezinciuc *et al.* 2014), and nuclear single sequence repeat microsatellite markers (Grandjean *et al.* 2014). Phylogenetic analyses using chitinase gene analyses (Makkonen *et al.* 2012a) and AFLP-PCR (Rezinciuc *et al.* 2014) indicate that all the strains of *A. astaci* split into two lineages: (i) one that comprises strains from RAPD-PCR groups A, B, C, and E, and (ii) a second one that comprises strains of RAPD-PCR group D. Furthermore, the chitinase gene sequencing and microsatellite markers have also been applied as a diagnostic tool to characterize the pathogen strains causing crayfish plague outbreaks (*e.g.*, Panteleit *et al.* 2017). However, the application of the chitinase gene as a marker has been found limited due to its incapability to separate the RAPD-PCR groups B and E (Makkonen *et al.* 2012a). For the microsatellites, the interpretation of the results is often hard due to the lack of possibility to confirm the amplification specificity and possible mixed infections from other Oomycetes species often present in crayfish (Kozubíková-Balcarová *et al.* 2013). Both methods also fail in cases when the pathogen quantities in samples are low, *i.e.*, the quantitative PCR (qPCR) shows agent levels of mid-A3 or lower (Vrålstad *et al.* 2009). Therefore, only a limited number of crayfish plague outbreak cases detected with qPCR can be further characterized with these applications.

The diversity, distribution, and prevalence of *A. astaci* in its original distribution area in North America are still largely unknown. When novel species or crayfish from North America were introduced to Europe, likely also *A. astaci* has been repeatedly introduced with these animals (Makkonen *et al.* 2012a; Jussila *et al.* 2015; Rezinciuc *et al.* 2015). Nowadays, this threat should be minimized due to the EU regulation 1143/2014 on invasive alien species. The origin and geographic migration of a broad variety of organisms, including oomycetes, have been tracked by using mitochondrial DNA (mtDNA) (Martin *et al.* 2007, 2008; Yoshida *et al.* 2013). When working with clonally reproducing organisms such as *A. astaci*, the mitochondrial (mt) genome provides a valuable marker for population studies (Makkonen *et al.* 2016). Thus, the

aim of this study was to examine the potential applicability of mtDNA as a tool to track the origin and diversity of the crayfish plague pathogen *A. astaci* and provide a basis for developing an efficient tool to further characterize the disease outbreaks and their origins. The *A. astaci* diversity in Europe, as well as in its original distribution in North America, are currently rather poorly known, but hopefully intensively studied also in the future. As critical differences in the pathogen strains' virulence properties in Europe have also been observed (e.g., Diéguez-Uribeondo *et al.* 1995; Makkonen *et al.* 2012b, 2014), the characterization of the strains causing the epidemics in the wild must be considered as a task with a high importance.

MATERIALS AND METHODS

Strains and species tested

A total of 27 *A. astaci* strains from the culture collections of the University of Eastern Finland (Finland), Evira (Finland), Charles University of Prague (Czech Republic), and Real Jardín Botánico-CSIC (Spain) were sequenced in this study. The strains were representing the five currently recognized RAPD-groups in Europe (Table 1). In addition, two Saprolegniales species, *Aphanomyces frigidophilus* and *Saprolegnia* sp., were sequenced as reference (Table 1).

Primer design

The annotated mt genome (KX405004) of *A. astaci* was used as a reference sequence for the primer design (Makkonen *et al.* 2016) and the regions containing group specific differences were selected based on alignments with *A. astaci* transcriptomic data produced at the University of Eastern Finland (Kokko *et al.* unpublished). The alignments and manual editions of the sequences were conducted in Geneious 8.0 (Kearse *et al.* 2012). Primers were designed with the Primer3 program (Rozen and Skaletsky, 2000). Two primer pairs amplifying the mitochondrial ribosomal rnsS (AphSSUF and AphSSUR) and rnsL (AphLSUF and AphLSUR) genes were designed (Table 2).

The species specificity of the target region was checked with sequence alignments to oomycetes that were either available in GenBank or sequenced in this study (Fig. 1ab). The species from GenBank were *Aphanomyces invadans* (KX405005), *Saprolegnia ferax* (AY534144), *Pythium insidiosum* (AP014838), *Phytophthora infestans* (AY898627), *P. ipomoeae* (HM590420), *P. mirabilis* (HM590421), *P. phaseoli* (HM590418), *P. polonica*

(KT946598), *P. ramorum* (DQ832718), *P. sojae* (DQ832717), *P. andina* (KJ408269), and *Pseudosperenospora cubensis* (KT072718).

PCR

The PCR reactions were carried out in 25 μ L reaction volume containing 1 U of DreamTaq DNA polymerase (Thermo Fisher Scientific), 2X DreamTaq Green master mix (Thermo Fisher Scientific), 10 mM of primers, and 10-100 ng of template DNA. The reaction volume was filled with PCR-grade water. The amplification was conducted on a PTC-200 thermal cycler (MJ Research) with the following conditions: 95 °C, 3 min, 35x (95 °C, 30 s; 59 °C, 30 s; 72 °C, 30 s), and 72 °C 10 min. Each run contained a positive control (*A. astaci* DNA of strain UEF8866-2) and a blank reaction without a template. The amplification was checked on a 1.5% agarose gel containing 0.5 μ M EtBr. Then, the samples were purified with GeneJET PCR Purification Kit (Thermo Fisher Scientific).

Sequencing, phylogenetics, and analysis on the genetic diversity

The Sanger sequencing reactions were performed in GATC Biotech (Germany) with the primers AphSSUF and AphLSUF, respectively (Table 2). Approximately half of the amplicons were confirmed by additional sequencing with appropriate reverse primers AphSSUR or AphLSUR. The resulting sequence data was manually revised and edited, and the low-quality reads filtered out from the alignments in Geneious version 8.0 (Kearse *et al.* 2012) and the primer sites were cut off from the sequences before the further analyses. The sequences were entered to NCBI GenBank database with access numbers MF973121-MF973149 for *rnnS* and MF975950-MF975978 for *rnnL*.

Two phylogenetic approximations, a Bayesian inference (BI) and a maximum likelihood (ML) analyses, and a distance method, a neighbor-joining distance based analyses (NJ), were employed to reconstruct the phylogenetic relationships. The BI was performed in Mr Bayes v.3.2.6 software (Ronquist *et al.* 2012) using the MCMC method with 10,000,000 generations, three runs (8 chains per run) with a burn-in of 25% trees and a standard deviation of split frequencies <0.01 . Nodes with posterior probability (pp) values ≥ 0.95 were considered supported. The ML was performed using RAxML v.8 (Stamatakis, 2014) implemented in raxmlGUI v1.5b1 (Silvestro and Michalak, 2012), with 100 independent replicates and 1000 rapid bootstraps. Nodes with bootstrap values ≥ 75 were considered supported. The NJ analysis for inferring the phylogeny was performed utilizing MEGA v6.06 (Tamura *et al.* 2013) using Kimura 2-parameter distances between the sequences and bootstrap values determined by 1000

replications. All the resulting trees from the BI, ML, and NJ were visualized on FigTree v1.4.2 (Rambaut, 2012). *A. frigidophilus* was used as an outgroup in all approximations. We performed the analyses for the independent rnnS and rnnL, as well as for the concatenated rnnS and rnnL regions with the same parameters described above.

Genetic diversity was estimated calculating the number of polymorphic (segregating) sites (S), the number of haplotypes, the haplotype diversity (Hd), the average number of nucleotide differences (k), and the nucleotide diversity (π) utilizing the program DNAsp v.5.10.01 (Librado and Rozas, 2009). We used TCS v.1.21 (Clement *et al.* 2002) to represent the mutational changes between the sequences throughout the most parsimonious haplotype network and to visualize the genealogical relationships, we used PopArt v1.7.2 (Leigh and Bryant, 2015).

Microsatellite genotyping

To validate the results of the mitochondrial data with the methods currently in use and obtain grouping for the previously uncharacterized strains, microsatellite analyses of selected strains (Table 1) were conducted at the University of Koblenz-Landau (Germany) utilizing the nine co-dominant microsatellite markers according to Grandjean *et al.* (2014). The PCR reactions were carried out with Multiplex PCR Kit (Qiagen, the Netherlands) and 0.1 to 0.38 μ M of each of the labeled primers Aast4, Aast6, Aast7, Aast14 for Batch A as well as Aast2 Aast9, Aast10, Aast12, Aast13 for Batch B were added. 1 μ L DNA template was appended for final volumes of 5 μ L and 5.5 μ L, respectively. The fragment analyses were conducted on a Beckman Coulter CEQ 8000 eight capillary sequencer. Alleles were scored using the GenMarker software (version 1.95, SoftGenetics LLC) and compared to reference strains.

Direct A. astaci haplotyping from infected crayfish cuticle samples

Direct haplotyping from infected crayfish samples was conducted at the University of Koblenz-Landau (Germany). One sample was from an aquarium-held marbled crayfish, *Procambarus fallax* f. *virginialis*, already tested positively for crayfish plague infection by Keller *et al.* (2014). Moreover, *A. astaci* DNA was extracted from stone crayfish belonging to populations from three natural water bodies in Austria and Germany, which underwent mass mortalities at the time of sampling (Table 3).

DNA of *A. astaci* was extracted from infected crayfish tissue using a CTAB method and the crayfish plague agent levels of them were examined with qPCR according to Vrålstad *et al.* (2009). The PCR reaction mixture contained 0.4 μ M of each primer (Table 2), 0.75X

DreamTaq Green master mix (Thermo Fisher Scientific), 0.5 U DreamTaq DNA polymerase (Thermo Fisher Scientific), 0.17 mM dNTPs, and 2.5 µl of the DNA template. The mixture was filled up to 12.5 µl with PCR-grade water. PCR was carried out on a Primus 96 Plus Thermal Cycler (PEQLAB Biotechnologies GmbH) with the following conditions: 95 °C, 3 min, 30x (95 °C, 30 s; 60 °C, 30 s; 72 °C, 30 s), and 72 °C 10 min. Each run contained a positive control (*A. astaci* DNA) and a blank reaction without a template. The amplification was checked on an agarose gel with EtBr labelling. The PCR products were sequenced on a 3730 DNA Analyzer eight capillary sequencer (Applied Biosystems) by the company Seq IT GmbH & Co. KG (Kaiserslautern, Germany). The sequences were aligned and edited using the program Geneious R7 (Kearse *et al.* 2012) and then entered to NCBI GenBank database with the access numbers MF150010-MF150017. Microsatellite analyses of infected crayfish samples were conducted similarly as explained in chapter 2.5.

RESULTS

Primer specificity

The two primer pairs developed to amplify the mitochondrial ribosomal rnnS and rnnL subunits (Table 2, Fig. 1) produced amplicons with lengths of 512 bp and 435 bp (with primer regions included) from the tested *A. astaci* strains, respectively.

The primer pair AphSSU (Table 2, Fig. 1A), developed for the rnnS subunit, also amplified some other aquatic oomycetes, *i.e.*, *Saprolegnia* sp. However, the species were later easily identified based on their nucleotide sequences, as the sequence alignments and BLAST comparisons of the 512 bp rnnS region showed the sequence diversity to be high enough to separate *A. astaci* from closely related species. The differences for rnnS were 16 nucleotides (97.0% similarity) to *A. frigidophilus*, and 35 nucleotides (93.0% similarity) to *Saprolegnia* sp. (see the details of the species in table 1). Furthermore, the BLAST search to NCBI GenBank showed 12 nucleotides (97.5% similarity) to *A. invadans* (KX405005) and a 93.3% similarity (32 nucleotides) to *Saprolegnia ferax* (AY534144).

The rnnL primers showed high species divergence at the primer regions (Fig. 1B). At the 435 bp rnnL region, the diversity was slightly more variable, showing 94.6% similarity (20 nucleotides) to *A. frigidophilus*, but up to 100% similarity was detected against *Saprolegnia* sp., although the similarity to another parasitic *Saprolegnia* having rnnL sequence available, *S. ferax* (AY534144), showed only 116 bp matching region with 99.0% similarity, this 116 bp

matching region was also observed for *A. invadans* (KX405005) with 97.4% similarity (3 nucleotides).

Intraspecific diversity, phylogeny, and genetic diversity

For the diversity estimations, a 475 bp and 391 bp fragments of *rnnS* and *rnnL* amplicons were included, respectively (Supplementary Fig. 1). The two phylogenetic approximations and the inferred method used to reconstruct the phylogenetic relationships (BI, ML, and NJ, respectively) (Fig. 2) supported the differentiation of two lineages for each of the data sets used in this study (*rnnS* alignment, *rnnL* alignment; and the concatenated *rnnS* and *rnnL* alignment): first lineage includes the A, B, C, and E RAPD-PCR groups and a second lineage is formed by D RAPD-PCR group (Fig. 2).

According to the phylogenetic analysis of the *rnnS* alignment (Fig. 2a), the first lineage includes only two subgroups. The first subgroup includes the sequences similar to the strains that belong to the RAPD-PCR groups A, C, and E; and the second subgroup includes the sequences similar to the strains that belong to the RAPD-PCR group B. The second lineage includes the sequences similar to the strains that belong to the RAPD-PCR groups D (Fig. 2a). In contrast, the phylogenetic analysis of the *rnnL* alignment includes two subgroups for the first lineage. The first subgroup is composed by similar sequences to the strains from the RAPD-PCR groups A, B, and C; and the second subgroup by similar sequences to the strains from the RAPD-PCR groups E, although the RAPD-PCR group E is not supported by the phylogenetic analyses. The second lineage includes the similar sequences to the strains that belong to the RAPD-PCR groups D (Fig. 2b).

As a result of the concatenated *rnnS* and *rnnL* sequences, we found three defined haplogroups within these two main lineages, grouping similar strains of the concatenated sequences *rnnS* and *rnnL* (Fig. 2c). Lineage 1 includes three haplogroups (A-, B-, and E-haplogroup), each represented by different specific haplotypes. The A-haplogroup is formed by strains from RAPD-PCR groups A and C, including only one haplotype, *i.e.*, a-haplotype. The a-haplotype comprises sequences from RAPD-PCR groups A, *i.e.*, L1 and Upor4, and sequences from RAPD-PCR group C, *i.e.*, Kv1 (Fig. 2c). The B-haplogroup is formed by strains from RAPD group B, *i.e.*, Pl, EviraK047/99, SAP-Pamplona, which comprises the unique b-haplotype. The E-haplogroup is formed by strains from RAPD-PCR groups E, including one haplotype, *i.e.*, e-haplotype Li10 (Fig. 2c). Lineage 2 includes only one haplogroup (D-haplogroup), confirmed

by strains from the RAPD-PCR group D, *i.e.*, AP03 and SAP-Málaga5. This D-haplogroup has two haplotypes, *i.e.*, d1-haplotype (with the sequence SAP-Málaga5) and d2-haplotype (with the genome sequenced sequence AP03) (Fig. 2c).

The genetic diversity analysis confirmed and supported the phylogenetic analysis. We found differences between the separated mitochondrial ribosomal *rnnS* and *rnnL* subunits (Fig. 3, Supplementary Table 1). The amplicons corresponding to the *rnnS* subunit only registered 2 segregating sites (S) leading to 3 different haplotypes (Fig. 3a). The haplotype diversity (Hd) was 0.598; with 0.744 average nucleotide differences (k) and a nucleotide diversity (π) of 0.0015. On the other hand, the amplicons corresponding to the *rnnL* subunit registered 8 segregating sites (S) leading to 4 different haplotypes (Fig. 3b). The haplotype diversity (Hd) was 0.297; with 1.415 average nucleotide differences (k) and a nucleotide diversity (π) of 0.004. However, the concatenated sequences *rnnS* and *rnnL* showed a total of 10 segregating sites (S; Supplementary figure 1), where 8 of them were parsimony informative, confirming the existence of a total of 5 haplotypes (Fig. 3c). The haplotype diversity (Hd) was 0.626; with 2.159 average nucleotide differences (k) and a nucleotide diversity (π) of 0.0025.

Direct haplotyping of infected crayfish samples

The specimens which showed the highest agent levels among the tested populations were selected for *A. astaci* haplotyping (Table 3). The qPCR agent levels of these successfully PCR amplified and sequenced samples varied between A5 and A7 (Table 3). The stone crayfish from the Schwarzbach (Germany) and the marbled crayfish sample (the Netherlands) were infected with the D-haplogroup of *A. astaci*. Here, the haplotype detected from the stone crayfish (GiSt5) was identical with the d1-haplogroup strain SAP-Málaga, while the DNA detected from marbled crayfish (IvoOkt13) grouped together with the d2-haplotype strain AP03 (Fig. 2c). The remaining two samples from stone crayfish, *i.e.*, populations from a feeder of the Steyr River (AUT2_1) and the Schädlnbach (StGM9) in Austria, belonged to the b-haplotype.

DISCUSSION

In this paper, we have described a mitochondrial PCR and sequencing based approach that allows identifying the genetic diversity of *A. astaci* in mix genome samples, *i.e.*, clinical and preserved samples. These mitochondrial markers are stable and reliable and the results are

easily repeatable in different laboratories with samples obtained from various crayfish host species revealing moderate to high infection levels.

The target regions *rnnS* and *rnnL* were selected based on the full mitochondrial genome of Spanish *A. astaci* strain AP03 (D-haplogroup) (Makkonen *et al.* 2016) and transcriptomics data of selected Finnish *A. astaci* strains representing the A- and B-haplogroups (Kokko *et al.* unpublished). The most commonly used mitochondrial barcoding gene (Hebert *et al.* 2003), Cytochrome Oxidase I (COI), contained no single nucleotide polymorphisms (SNPs) to distinguish the different *A. astaci* strains and was therefore left out from further analyses and method development. Furthermore, a very low GC-content of the mtDNA, especially in the intergenic regions (Makkonen *et al.* 2016), and lacking data from intergenic regions limited the possible target regions for mtDNA haplotyping.

The specificity tests of the two primer pairs showed that the species level resolution of the mitochondrial ribosomal subunits (*rnnS* and *rnnL*) was high enough to separate closely related *Aphanomyces* species, *i.e.*, *A. invadans* and *A. frigidophilus*, from *A. astaci*. The *rnnL* region exhibited higher specificity, although the overall sequence diversity of the whole PCR amplicon was more variable. However, a single *Saprolegnia* sp. showed 100% sequence similarity with *A. astaci*. Therefore, sequencing the *rnnL* region alone for species differentiation cannot be recommended. The *rnnS* region also amplified other aquatic oomycetes, such as *A. hypogyna* and *Saprolegnia* sp., but the species could be later separated based on the sequence data.

The method functionality was also compared to the microsatellite method developed by Grandjean *et al.* (2014). We conducted parallel analyses for studied *A. astaci* strains (Table 1) and infected clinical samples from infected crayfish (Table 3), and they grouped similarly with both methods. In some cases, when the agent levels detected in qPCR (Vrålstad *et al.* 2009) were mid-A3 or higher, the mtDNA markers showed slightly more sensitive amplification in comparison to the microsatellite markers (data not shown). The difference in the amplification sensitivity was likely caused by different copy number of the mtDNA in comparison to the nuclear DNA analyzed with the microsatellite markers. In future, the application of DNA extraction methods favoring the recovery of circular (mitochondrial) DNA for crayfish tissues will likely further increase the usability of the mtDNA markers in comparison to microsatellites. On the other hand, the diversity of *A. astaci* observed using our mtDNA markers was lower in comparison to the microsatellite markers. Here, the mtDNA markers were highly stable overall, the interpretation of the results from sequencing data was objective.

Especially if new or unexpected species and strains will be detected, sequencing can be considered as the best choice to confirm the results in the aquatic environment with unknown microbial spectrum and diversity.

The phylogenetic and genetic diversity analyses of the two concatenated regions of the mitochondrial ribosomal subunits analyzed, *i.e.*, *rnnS* and *rnnL*, based on reference strains of the groups (*i.e.*, L1 for RAPD-PCR group A, Pl for RAPD-PCR group B, Kv1 for RAPD-PCR group C, AP03 for RAPD-PCR group D, and Li10 for RAPD-PCR group E) showed similar results to those obtained by previous studies (Huang *et al.* 1994; Dieguez-Uribeondo *et al.* 1995; Kozubíková *et al.* 2011; Grandjean *et al.* 2014; Rezinziuc *et al.* 2014). Thus, these analyses allowed the identification of two main lineages and four haplogroups. Three of these haplogroups (*i.e.*, B-haplogroup, D-haplogroup, and E-haplogroup) corresponded to RAPD-PCR groups B, D, and E, and the fourth-one, *i.e.*, A-haplogroup, comprised the strains from group RAPD-PCR A and C. Each haplogroup was characterized by having a single, unique haplotype, except for the D-haplogroup that possessed two haplotypes, *i.e.*, d1 and d2. Therefore, the combination of both markers led us to clearly separate four haplogroups (A, B, D, and E) with five different haplotypes in them (a, b, d1, d2, and e).

The A-haplogroup and E-haplogroup were closely related haplogroups, although the haplotype network showed two SNPs between the groups of concatenated sequences. The number of isolates available from the E-haplogroup is currently limited (Kozubíková *et al.* 2011; Kozubíková-Balcarová *et al.* 2013). Moreover, the A-haplogroup comprise sequences identical to the strain of reference for RAPD groups A (L1 strain) and C (Kv1 strain). The haplotype network generated no differences between these groups. Although this fact can be important and should be taken into account in the investigations, only one strain of *A. astaci* belonging to RAPD-PCR group C has been isolated so far (Huang *et al.* 1994; Kenneth Söderhäll, personal communication). Therefore, the limitation of strains corresponding to the RAPD-PCR groups C and E (Kozubíková *et al.* 2011) could have hindered the estimation of the real diversity within these haplogroups. Alternatively, the limited number of variable sites in the genetic regions used here did not offer possibilities to discriminate these RAPD-PCR groups.

The *A. astaci* isolates for the A-haplogroup and E-haplogroup were obtained from several host species (Table 1) from Eastern and Northern USA, *i.e.*, genera *Orconectes* and genus *Pacifastacus*. However, Eastern and Northern parts of USA have broad and variable crayfish species diversities (Holdich, 2002). The host diversity likely increases also the pathogen strain diversity and accelerates the development of new lineages, haplogroups, and haplotypes, as a

consequence of host-parasite coevolution (Jussila *et al.* 2015). Moreover, the translocation of species within North America occurs (Larson *et al.* 2012). For example, three *P. leniusculus* subspecies have been introduced in Lake Tahoe (John Umek, personal communication). The results observed here may be an indication of those crayfish translocations. Furthermore, it can be assumed that also mixed crayfish species populations have been created with this kind of translocations. Although no evidence of this has been shown so far, these translocations could have allowed the pathogen host jumps, making possible the exchange of genetic groups (*e.g.*, Jussila *et al.* 2015). However, to investigate this possibility, further isolations from North American crayfish should be performed. In this kind of cases, using microsatellites would not be helpful, as distinguishing between a truly heterozygous locus or a combination of two different strains is impossible (Maguire *et al.* 2016). On the other hand, the mixture of pathogen strains might already be reality in Europe since several non-indigenous crayfish species, several members of the genus *Orconectes* as an example, have been introduced into Europe (Souty-Grosset *et al.* 2006), especially into Central European water bodies (Schrimpf *et al.* 2013; Panteleit *et al.* 2017). The oldest known *A. astaci* lineage in Europe, *i.e.*, RAPD-PCR group A was the basis of the a-haplotype in this study. If the RAPD-PCR group A of *A. astaci*, with its so far unknown original crayfish host, first arrived in Europe in the ballast water of an intercontinental ship, as speculated by Alderman (1996), the East coast of North America was the likely origin for the transport. Therefore, our results seem to be in line with these speculations.

The B-haplogroup, commonly detected all over Europe due to signal crayfish *P. leniusculus* introductions, can be traced back to California (Souty-Grosset *et al.* 2006). Signal crayfish were first introduced to Europe from several Californian sources. Lake Tahoe is being mentioned as the main source of introductions in several papers (Abrahamsson, 1969, 1972; Westman, 1972, 2000; Goldman, 1972; Agerberg and Jansson, 1995). In addition, Lake Hennessey and Sacramento River were mentioned as sources of introduction in Finland (Westman, 2000) as well as Donner Lake, American River and Pitt Lake in Sweden (Agerberg and Jansson, 1995). Based on this study, either the signal crayfish from these locations were either carrying similar strains of *A. astaci*, or the stocking success of some of these populations was limited creating a founder effect (Agerberg and Jansson, 1995), as the all b-haplotype strains examined here were identical with the recent isolates from Lake Tahoe (Table 1). Homogeneity within B-haplogroup has also been previously detected in nuclear markers (Diéguez-Uribeondo *et al.* 2009; Makkonen *et al.* 2011, 2012a).

The D-haplogroup seems to be introduced to Southern Europe (Spain) by introductions of *P. clarkii* (Rezinciuc *et al.* 2014). However, only two strains were tested in this study. The two Spanish *A. astaci* strains, SAP-Málaga and AP03, split the D-haplogroup into two haplotypes, d1 and d2, respectively. Variation in this group was also observed with the microsatellite markers (unpublished data), where the first Pc-lineage has been typically connected to *P. clarkii* and the second one to marbled crayfish *P. fallax* f. *virginalis*, a parthenogenetic species commonly available in the aquarium trade (*e.g.*, Scholtz *et al.* 2003; Panteleit *et al.* 2017). In this study, the D-haplogroup mtDNA markers, which were detected from an infected crayfish tissue (Table 3), were exhibiting a similar grouping as the strains AP03 and SAP-Málaga, showing that both haplotypes are present in Spain and Germany (Fig. 2).

The application of mitochondrial markers enables now the direct identification in clinical and preserved samples of the main *A. astaci* haplogroups responsible for crayfish plague outbreaks. The method provides an opportunity to characterize the diversity of *A. astaci* strains, facilitating investigations on disease history and its epidemiology. In this paper, we have described the technique's possibilities for a direct identification of *A. astaci*, responsible of the crayfish plague, which is still discovered in novel regions causing devastating outbreaks (*e.g.*, Peiró *et al.* 2016). We propose these mitochondrial rnnS and rnnL markers as an important tool to track and understand the *A. astaci* diversity and evolution among the original host species, *i.e.*, North American crayfish species, and in the future, it may help to define if the original distributional area of *A. astaci* groups is a reflection to its original host species distribution and North America.

ACKNOWLEDGEMENTS

Thanks to Adam Petrusek, Charles University of Prague, Czech Republic, for providing the strains Li10 and Upor4, Satu Viljamaa-Dirks, Evira, Finland, for *A. astaci* strain K047/99 and Ivo Roessink, Wageningen University and Research, Netherlands, for marbled crayfish samples.

FINANCIAL SUPPORT

This research has been supported by the strategic funding of the University of Eastern Finland (Innovative Research Initiatives), LIFE+ CrayMate (LIFE12 INF/FI/233), Finnish Cultural Foundation, and Maj and Tor Nessling Foundation.

REFERENCES

- Abrahamsson, S.** (1969). Signal kräftan — erfarenheter från USA och aspekter på dess inplantering i Sverige. *Fauna och Flora* **64**, 109–116. In Swedish.
- Abrahamsson, S.**, (1972). The crayfish *Astacus astacus* L. in Sweden and the introduction of the American crayfish *Pacifastacus leniusculus*. *Freshwater Crayfish* **1**, 27–40.
- Agerberg, A., and Jansson, H.** (1995). Allozymic comparisons between three subspecies of the freshwater crayfish *Pacifastacus leniusculus* (Dana), and between populations introduced to Sweden. *Hereditas* **122(1)**, 33–39. doi:10.1111/j.1601-5223.1995.00033.x
- Alderman, D.J.** (1996). Geographical spread of bacterial and fungal diseases of crustaceans. *Scientific and Technical Review of the Office International des Epizooties (Paris)* **15**, 603–632.
- Cerenius, L., Andersson, M.G. and Söderhäll, K.** (2009). *Aphanomyces astaci* and Crustaceans. In *Oomycete genetics and genomics: diversity, interactions, and research tools* (eds. Lamour, K. and Kamoun, S.), pp. 425–433. John Wiley & Sons, Inc., Hoboken, NJ, USA. doi: 10.1002/9780470475898.
- Clement, M., Posada, D. and Crandall, K. A.** (2000). TCS: a computer program to estimate gene genealogies. *Molecular Ecology* **9(10)**, 1657–1660. doi: 10.1046/j.1365-294x.2000.01020.x.
- Diéguez-Uribeondo, J. and Söderhäll, K.** (1993). *Procambarus clarkii* Girard as a vector for the crayfish plague fungus, *Aphanomyces astaci* Schikora. *Aquaculture and Fisheries Management* **24**, 761–765. doi: 10.1111/j.1365-2109.1993.tb00655.x.

- Diéguez-Uribeondo, J., Huang, T.S. and Cerenius, L.** (1995). Physiological adaptation of an *Aphanomyces astaci* strain isolated from the freshwater crayfish *Procambarus clarkii*. *Mycological Research* **99**, 574–578. doi: 10.1016/S0953-7562(09)80716-8.
- Diéguez-Uribeondo, J., Garcia, M.A., Cerenius, L., Kozubíková, E., Ballesteros, I., Windels, C., Weiland, J., Kator, H., Söderhäll, K. and Martin, M.P.** (2009). Phylogenetic relationships among plant and animal parasites, and saprotrophs in *Aphanomyces* (Oomycetes). *Fungal Genetics and Biology* **46**, 365–376. doi: 10.1016/j.fgb.2009.02.004.
- Goldman, C.R.,** (1972). Ecology and physiology of the Californian crayfish *Pacifastacus leniusculus* (Dana) in relation to its suitability for introduction into European waters. *Freshwater Crayfish* **1**, 105–120.
- Grandjean, F., Vrålstad, T., Diéguez-Uribeondo, J., Jelić, M., Mangombi, J., Delaunay, C., Filipová, L., Rezinciuc, S., Kozubíková-Balcarová, E., Guyonnet, D., Viljamaa-Dirks, S. and Petrussek, A.,** (2014). Microsatellite markers for direct genotyping of the crayfish plague pathogen *Aphanomyces astaci* (oomycetes) from infected host tissues. *Veterinary Microbiology* **170(3-4)**, 317–324. doi: 10.1016/j.vetmic.2014.02.020.
- Hebert, Paul D.N., Ratnasingham, S. and Waard, R.D.** (2003). Barcoding animal life: cytochrome c oxidase subunit 1 divergences among closely related species. *Proceedings of the Royal Society of London Series B Biological sciences* **270 (1)**, 96–99. doi:10.1098/rsbl.2003.0025.
- Holdich, D.M.** 2002. *Biology of freshwater crayfish*. Blackwell Science, Oxford, UK.

- Huang, T.S., Cerenius, L. and Söderhäll, K.** (1994). Analysis of genetic diversity in the crayfish plague fungus, *Aphanomyces astaci*, by random amplification of polymorphic DNA. *Aquaculture* **126**, 1–9. doi: 10.1016/0044-8486(94)90243-7.
- International Union For Conservation of Nature (IUCN)**, (2012). *The IUCN red list of threatened species*. Version 2012.2. <<http://www.iucnredlist.org>> (accessed 11.04.17)
- Jussila, J., Vrezec, A., Makkonen, J., Kortet, R. and Kokko, H.** (2015). Invasive crayfish and their invasive diseases in Europe with the focus on the virulence evolution of the crayfish plague. In *Biological invasions in changing ecosystems. Vectors, ecological impacts, management and predictions* (ed. Canning-Clode, J.), pp. 183–211. De Gruyter Ltd, Warsaw, Poland.
- Jussila, J., Vrezec, A., Jaklič, T., Kukkonen, H., Makkonen, J. and Kokko, H.** (2017). Virulence of *Aphanomyces astaci* isolate from latently infected stone crayfish (*Austropotamobius torrentium*) population. *Journal of Invertebrate Pathology* **149**, 15–20. doi: 10.1016/j.jip.2017.07.003.
- Kearse, M., Moir, R., Wilson, A., Stones-Havas, S., Cheung, M., Sturrock, S., Buxton, S., Cooper, A., Markowitz, S., Duran, C., Thierer, T., Ashton, B., Meintjes, P. and Drummond, A.** (2012). Geneious Basic: an integrated and extendable desktop software platform for the organization and analysis of sequence data. *Bioinformatics* **28(12)**, 1647–1649. doi: 10.1093/bioinformatics/bts199.
- Keller, N.S., Pfeiffer M., Roessink, I., Schulz, R. and Schrimpf, A.**, (2014). First evidence of crayfish plague agent in populations of the marbled crayfish (*Procambarus fallax* forma *virginalis*). *Knowledge and Management of Aquatic Ecosystems* **414**, 15. doi: 10.1051/kmae/2014032.

- Kozubíková, E., Viljamaa-Dirks, S., Heinikainen, S. and Petrusek, A.** (2011). Spiny-cheek crayfish *Orconectes limosus* carry a novel genotype of the crayfish plague pathogen *Aphanomyces astaci*. *Journal of Invertebrate Pathology* **108**, 214–216. doi: 10.1016/j.jip.2011.08.002.
- Kozubíková-Balcarová, E., Koukol, O., Martín, M. P., Svoboda, J., Petrusek, A. and Diéguez-Uribeondo, J.** (2013). The diversity of oomycetes on crayfish: Morphological vs. molecular identification of cultures obtained while isolating the crayfish plague pathogen. *Fungal Biology* **117(10)**, 682–691. doi: 10.1016/j.funbio.2013.07.005.
- Larson, E.R., Abbot, C., Usio, N., Azuma, N., Wood, K., Herborg, L.M. and Olden, J.D.** (2012). The signal crayfish is not a single species: cryptic diversity and invasions in the Pacific Northwest range of *Pacifastacus leniusculus*. *Freshwater Biology* **57(9)**, 1823–1838. doi: 10.1111/j.1365-2427.2012.02841.x.
- Leigh, J.W. and Bryant, D.** (2015). POPART: full-feature software for haplotype network construction. *Methods in Ecology and Evolution* **6(9)**, 1110–1116. doi: 10.1111/2041-210X.12410.
- Librado, P. and Rozas, J.** (2009). DnaSP v5: a software for comprehensive analysis of DNA polymorphism data. *Bioinformatics* **25**, 1451–1452. doi: 10.1093/bioinformatics/btp187.
- Lowe, S., Browne, M., Boudjelas, S. and De Poorter, M.** (2004). *100 of the world's worst invasive alien species: a selection from the global invasive species database*. The invasive species specialist group (ISSG), a specialist group of the species survival commission (SSC) of the world conservation union (IUCN), Auckland, New Zealand.

- Maguire, I., Jelić, M., Klobučar, G., Delpy, M., Delaunay, C. and Grandjean, F.** (2016). Prevalence of the pathogen *Aphanomyces astaci* in freshwater crayfish populations in Croatia. *Diseases of Aquatic Organisms* **118(1)**, 45–53. doi: 10.3354/dao02955.
- Makkonen, J., Jussila, J., Henttonen, P. and Kokko, H.** (2011). Genetic variation in the ribosomal internal transcribed spacers of *Aphanomyces astaci* Schikora from Finland. *Aquaculture* **311**, 48–53. doi: 10.1016/j.aquaculture.2010.11.019.
- Makkonen, J., Jussila, J. and Kokko, H.** (2012a). The diversity of the pathogenic Oomycete (*Aphanomyces astaci*) chitinase genes within the genotypes indicate adaptation to its hosts. *Fungal Genetics and Biology* **49**, 635–642. doi: 10.1016/j.fgb.2012.05.014.
- Makkonen, J., Jussila, J., Kortet, R., Vainikka, A. and Kokko, H.** (2012b). Differing virulence of *Aphanomyces astaci* isolates and elevated resistance of noble crayfish *Astacus astacus* against crayfish plague. *Diseases of Aquatic Organisms* **102**, 129–136. doi: 10.3354/dao02547.
- Makkonen, J., Kokko, H., Vainikka, A., Kortet, R. and Jussila, J.** (2014). Dose-dependent mortality of the noble crayfish (*Astacus astacus*) to different strains of the crayfish plague (*Aphanomyces astaci*). *Journal of Invertebrate Pathology* **115(1)**, 86–91. doi: 10.1016/j.jip.2013.10.009.
- Makkonen, J., Vesterbacka, A., Martin, F., Jussila, J., Diéguez-Uribeondo, J., Kortet, R. and Kokko, H.** (2016). Mitochondrial genomes and comparative genomics of *Aphanomyces astaci* and *Aphanomyces invadans*. *Scientific Reports* **6**, 36089. doi: 10.1038/srep36089.
- Martin, M.D., Cappellini, E., Samaniego, J.A., Zepeda, M.L., Campos, P.F., Seguin-Orlando, A., Wales, N., Orlando, L., Ho, S.Y., Dietrich, F.S., Mieczkowski, P.A., Heitman, J., Willerslev, E., Krogh, A., Ristaino, J.B. and Gilbert, M.T.P.** (2013).

Reconstructing genome evolution in historic samples of the Irish potato famine pathogen. *Nature Communications* **4**, 2172.

Martin, M.D., Ho, S.Y.H., Wales, N., Ristaino, J.B. and Gilbert, T.P. (2014). Persistence of the mitochondrial lineage responsible for the Irish potato famine in extant new world *Phytophthora infestans*. *Molecular Biology and Evolution* **31**, 1414–1420. doi: 10.1093/molbev/msu086.

Panteleit, J., Keller, N.K., Kokko, H., Jussila, J., Makkonen, J., Theissing, K. and Schrimpf, A. (2017). Investigation of ornamental crayfish reveals new carrier species of the crayfish plague pathogen (*Aphanomyces astaci*). *Aquatic Invasions* **12(1)**, 77–83. doi: 10.3391/ai.2017.12.1.08.

Peiró, D.F., Almerão, M.P., Delaunay, C., Jussila, J., Makkonen, J., Bouchon, D., Araujo, P.B. and Souty-Grosset, C. (2016). First detection of the crayfish plague pathogen *Aphanomyces astaci* in South America: a high potential risk to native crayfish. *Hydrobiologia* **781(1)**, 181–190. doi: 10.1007/s10750-016-2841-4.

Rambaut, A. (2012). FigTree_v1.4.0. Available from: <http://tree.bio.ed.ac.uk/software/figtree/> [cited 29. September 2017].

Rezinciuc, S., Galindo, J., Montserrat, J. and Diéguez-Uribeondo, J. (2014). AFLP-PCR and RAPD-PCR evidences of the transmission of the pathogen *Aphanomyces astaci* (oomycetes) to wild populations of European crayfish from the invasive crayfish species, *Procambarus clarkii*. *Fungal Biology* **118(7)**, 612–620. doi: 10.1016/j.funbio.2013.10.007.

Rezinciuc, S., Sandoval-Sierra, J., Oidtmann, B. and Diéguez-Uribeondo, J. (2015). The biology of crayfish plague pathogen *Aphanomyces astaci*: current answers to most

frequent questions. In *Freshwater Crayfish* (eds. Kawai, T., Faulkes, Z. and Scholtz, G.), pp. 182–204. CRC Press, San Diego, USA. doi: 10.1201/b18723-1.

Ronquist, F., Teslenko, M., van der Mark, P., Ayres, D.L., Darling, A., Höhna, S., Larget, B., Liu, L., Suchard, M.A. and Huelsenbeck, J.P. (2012). MrBayes 3.2: Efficient Bayesian phylogenetic inference and model choice across a large model space. *Systematic Biology* **61(3)**, 539–542. doi: 10.1093/sysbio/sys029.

Rozen, S. and Skaletsky, H. (2000). Primer3 on the WWW for general users and for biologist programmers. *Methods in Molecular Biology* **132**, 365–386.

Schrimpf, A., Chucholl, C., Schmidt, T. and Schulz, R. (2013). Crayfish plague agent detected in populations of the invasive North American crayfish *Orconectes immunis* (Hagen, 1870) in the Rhine River, Germany. *Aquatic Invasions* **8(1)**, 103–109. doi: 10.3391/ai.2013.8.1.12.

Scholtz, G., Braband, A., Tolley, L., Reimann, A., Mittmann, B., Lukhaup, C., Steuerwald, F. and Vogt, G. (2003). Ecology: Parthenogenesis in an outsider crayfish. *Nature* **421**, 806. doi: 10.1038/421806a.

Silvestro, D. and Michalak, I. (2012). raxmlGUI: a graphical front-end for RAxML. *Organisms Diversity & Evolution* **12**, 335–337. doi: 10.1007/s13127-011-0056-0.

Souty-Grosset, C., Holdich, D.M., Noël, P.Y., Reynolds, J. and Haffner, P. (2006). *Atlas of crayfish in Europe*. Muséum National d'Histoire Naturelle, Paris; France.

Stamatakis, A. (2014). RAxML version 8: a tool for phylogenetic analysis and post-analysis of large phylogenies. *Bioinformatics* **30(9)**, 1312–1313. doi: 10.1093/bioinformatics/btu033.

Söderhäll, K. and Cerenius, L. (1999). The crayfish plague fungus: history and recent advances. *Freshwater Crayfish* **12**, 11–35.

- Tamura, K., Stecher, G., Peterson, D., Filipski, A. and Kumar, S. (2013).** MEGA6: Molecular evolutionary genetics analysis version 6.0. *Molecular Biology and Evolution* **30(12)**, 2725–2729. doi: 10.1093/molbev/mst197.
- Westman, K., (1972).** The population of the crayfish *Astacus astacus* L. in Finland and the introduction of the American crayfish *Pacifastacus leniusculus* Dana. *Freshwater Crayfish* **1**, 41–55.
- Westman, K. (2000).** *Comparison of the crayfish Pacifastacus leniusculus Dana, a species introduced into Finland, with the native species, Astacus astacus L., in allopatry and sympatry.* PhD thesis, University of Helsinki, Helsinki, Finland.
- Vrålstad, T., Knutsen, A.K., Tengs, T. and Holst-Jensen, A. (2009).** A quantitative TaqMan^(R) MGB real-time polymerase chain reaction based assay for detection of the causative agent of crayfish plague *Aphanomyces astaci*. *Veterinary Microbiology* **137**, 146–155. doi: 10.1016/j.vetmic.2008.12.022.
- Yoshida, K., Schuenemann, V.J., Cano, L.M., Pais, M., Mishra, B., Sharma, R., Lanz, C., Martin, F., Kamoun, S., Krause, J., Thines, M., Weigel, D. and Burbano, H. (2013).** The rise and fall of the *Phytophthora infestans* lineage that triggered the Irish potato famine. *eLife* **2**, e00731. doi: 10.7554/eLife.00731.

Table 1. The *Aphanomyces astaci* strains sequenced in this study. The strains considered as reference strains for each genotype based on RAPD and microsatellite results are bolded. na indicates no result available for RAPD genotype.

Strain code ^a	Origin	Isol. year	RAPD group ^c	Microsat. genotype ^d	Mitoch. haplotype	Host	Reference
L1	Lake Ämmern, SE	1962	A (As)	SSR-A₁	a	<i>A. astacus</i>	Huang et al. (1994)
Upor4	Úpořský brook, CZ	2005	na	SSR-Up	a	<i>A. torrentium</i>	Grandjean et al. (2014)
UEF_AT1D	River Borovniščica, SI	2014	na	SSR-A ₁	a	<i>A. torrentium</i>	Jussila et al. (2017)
UEF_VEN5/14	Lake Venesjärvi, Karvia, FI	2014	na	SSR-A ₁	a	<i>A. astacus</i>	Makkonen et al. (unpublished)
UEF_T2B	River Kemijoki, Taivalkoski, FI	2007	na	SSR-A ₁	a	<i>A. astacus</i>	Makkonen et al. (2012)
UEF_OI-1 (3)	Oxbow lake of River Rhine, Speyer, DE	2015	na	SSR-E	a	<i>O. immunis</i>	Makkonen et al. (unpublished)
Kv1 (VI03558)	Lake Pitt, CAN (SE)^b	1978	C (PsII)	SSR-C	a	<i>P. leniusculus</i>	Huang et al. (1994)
PI	Lake Tahoe, USA	1970	B (PsI)	SSR-B	b	<i>P. leniusculus</i>	Huang et al. (1994)
EviraK047/99	Lake Korpijärvi, Mäntyharju, FI	1999	B (PsI)	SSR-B	b	<i>A. astacus</i>	Viljamaa-Dirks et al. (2013)
UEF_8866-2	Lake Puujärvi, Karjalohja, FI	2003	B (PsI)	SSR-B	b	<i>P. leniusculus</i>	Makkonen et al. (2012)
UEF_SATR (2)	Lake Saimaa, FI	2012	na	SSR-B	b	<i>P. leniusculus</i>	Jussila et al. (2013)
UEF_KTY3-4	Fish Research Unit, Kuopio, FI	2008	na	SSR-B	b	<i>A. astacus</i>	Makkonen et al. (unpublished)
UEF_T16 (3)	Lake Tahoe, CA, USA	2013	na	SSR-B	b	<i>P. leniusculus</i>	Makkonen et al. (unpublished)
UEF_7203 (3)	Lake Kukkia, Luopioinen, FI	2003	B (PsI)	SSR-B	b	<i>P. leniusculus</i>	Makkonen et al. (2012)
UEF_8140 (2)	Lake Pyhäjärvi, Säskylä, FI	2003	B (PsI)	SSR-B	b	<i>P. leniusculus</i>	Makkonen et al. (2012)
SAP-Pamplona	Pamplona, ES		B (PsI)	SSR-B	b	<i>A. pallipes</i>	Martin-Torrijos et al. (unpublished)
AP03	Cataluña, ES	2013	D (Pc)	SSR-D	d1	<i>P. clarkii</i>	Rezinciuc et al. (2014)
SAP-Málaga5	Malaga, ES		D (Pc)	SSR-D	d2	<i>P. clarkii</i>	Martin-Torrijos et al. (unpublished)
Li10	Litavka River, CZ	2011	E (Or)	SSR-E	e	<i>A. astacus</i>	Kozubíková-Balcarova et al. (2013)
T16-JR26A	<i>Saprolegnia</i> sp.						Makkonen et al. (unpublished)
SAP817	<i>Aphanomyces frigidophilus</i>						Diéguez-Urbeondo et al. (2009)

^a With *n* of isolates sequenced from same location given in brackets.

^b Isolated in Sweden from signal crayfish which originated from Pitt Lake, Canada.

^c RAPD-genotypes published in Huang et al. (1994), Diéguez-Urbeondo et al. (1995), and Viljamaa-Dirks et al. (2013).

^d Microsatellite genotypes published by Grandjean et al. (2014).

Table 2. The primers.

Primer name	Sequence 5'-3'	Start pos.	Stop pos.	Length	Direction	%GC	T_m
AphSSUF	AGCACTCCGCCTGAAGAGTA	806	825	20	forward	55.0	60.6
AphSSUR	GGGCGGTGTGTACAAAGTCT	1 318	1 337	20	reverse	55.0	60.3
AphLSUF	AGGCGAAAGCTTACTATGATGG	2 849	2 870	22	forward	45.5	58.3
AphLSUR	CCAATTCTGTGCCACCTTCT	3 284	3 303	20	reverse	50.0	58.1

For Peer Review

Table 3. Samples sequenced directly from crayfish tissue.

Sample code	Species	Origin	Year	Crayfish (n)	Agent level ^a	Microsat. genotype ^b	Mitoch. haplotype	Reference
AUT2_1	<i>A. torrentium</i>	Feeder of the Steyr Fluss, Austria	2013	7	A7	SSR-B	b	–
StGM9	<i>A. torrentium</i>	Schädlbach, Austria	2014	17	A7	SSR-B	b	–
IvoOkt13	<i>P. fallax</i> f. <i>virginalis</i>	Aquarium-held crayfish, the Netherlands	2014	33	A5	SSR-D	d1	Keller et al. (2014)
GiSt5	<i>A. torrentium</i>	Schwarzbach, Germany	2013	16	A7	SSR-D	d2	–

^aThe highest agent level (according to Vrålstad et al. (2009)) detected among population, from which the haplotyping was conducted.

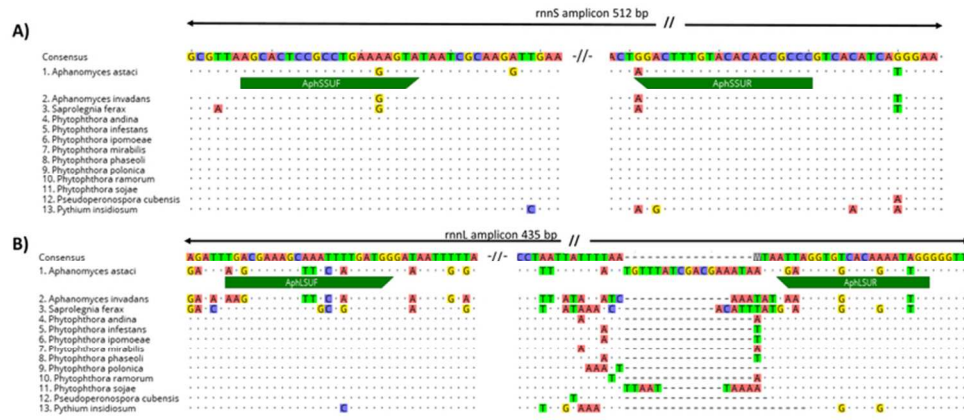
^bMicrosatellite genotypes identified using the method published by Grandjean et al. (2014).

For Peer Review

Figure 1. Primer regions aligned with other available oomycetes. A) rnnS region and primers AphSSUF and AphSSUR. B) rnnL-region and primers AphLSUF and AphLSUR.

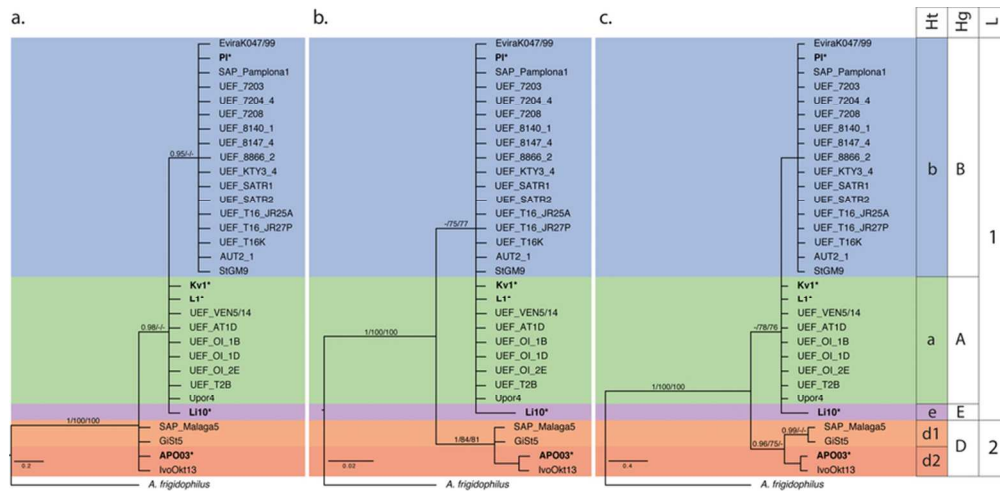
Figure 2. Bayesian inference analyses based on rnnS, rnnL, and concatenated rnnS + rnnL mtDNA sequences. **a.** Bayesian inference analysis was based on rnnS mtDNA sequences. **b.** Bayesian inference analysis was based on rnnL mtDNA sequences. **c.** Bayesian inference analysis was based on concatenated rnnS + rnnL mtDNA sequences. Values above the branches represent the posterior probabilities (>0.95) from Bayesian inference, and bootstrap support (> 75) from Maximum Likelihood and Neighbour Joining analyses. Scales bar for phylogenetic analysis indicates substitutions per site. The original strains used as references and identified in previous studies by RAPD-PCR technique appear in bold and with a star key (*), correspond to group A: L1*, group B: P1*, group C: Kv1*, group D: AP03*, group E: Li10*. Ht indicates haplotypes, Hp indicates haplogroups and L indicates lineages.

Figure 3. Haplotype network based on rnnS, rnnL, and concatenated rnnS + rnnL mtDNA sequences, generated by statistical parsimony. The area of the circles is proportional to the sequences number. **a.** Haplotype network based on rnnS mtDNA sequences. **b.** Haplotype network based on rnnL mtDNA sequences. **c.** Haplotype network based on concatenated rnnS + rnnL mtDNA sequences. Mutation steps between haplotypes are shown as hatch marks.



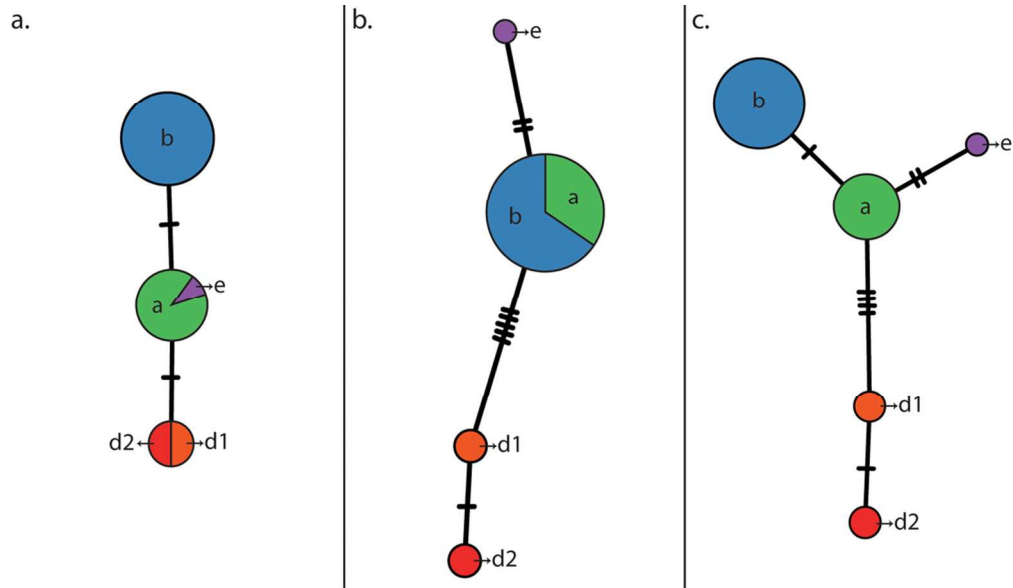
71x30mm (300 x 300 DPI)

Peer Review



Bayesian inference analyses based on *rnsS*, *rnnL*, and concatenated *rnsS* + *rnnL* mtDNA sequences. a. Bayesian inference analysis was based on *rnsS* mtDNA sequences. b. Bayesian inference analysis was based on *rnnL* mtDNA sequences. c. Bayesian inference analysis was based on concatenated *rnsS* + *rnnL* mtDNA sequences. Values above the branches represent the posterior probabilities (>0.95) from Bayesian inference, and bootstrap support (> 75) from Maximum Likelihood and Neighbour Joining analyses. Scales bar for phylogenetic analysis indicates substitutions per site. The original strains used as references and identified in previous studies by RAPD-PCR technique appear in bold and with a star key (*), correspond to group A: L1*, group B: PI*, group C: Kv1*, group D: APO3*, group E: Li10*. Ht indicates haplotypes, Hg indicates haplogroups and L indicates lineages.

80x39mm (300 x 300 DPI)



Haplotype network based on *rnnS*, *rnnL*, and concatenated *rnnS* + *rnnL* mtDNA sequences, generated by statistical parsimony. The area of the circles is proportional to the sequences number. a. Haplotype network based on *rnnS* mtDNA sequences. b. Haplotype network based on *rnnL* mtDNA sequences. c. Haplotype network based on concatenated *rnnS* + *rnnL* mtDNA sequences. Mutation steps between haplotypes are shown as hatch marks.

96x56mm (300 x 300 DPI)

Supplementary Figure 1. The multiple alignment of the rnsS (1-475 bp) and rnsL (476-867 bp) regions.

For Peer Review

Consensus
 SAP817 *Aphanomyces frigidophilus*
 APO03
 Iwo0113
 SAP-Malaga5
 GiS5
 Kv1
 L10
 L1
 UEF_VEN5/14
 UEF_AT1D
 UEF_Oh1B
 Udon4
 UEF_T2B
 UEF_Oh1D
 UEF_Oi2E
 SIGM9
 AUT2_1
 UEF_T16K
 UEF_T16-R27P
 UEF_T16-R25A
 UEF_SATR2
 UEF_SATR1
 UEF_KY3-3
 UEF_8866-2
 UEF_8147-4
 UEF_8140-1
 UEF_7208
 UEF_7204-4
 UEF_7203
 SAP-Pamplona1
 EsviraK047/99
 Pl

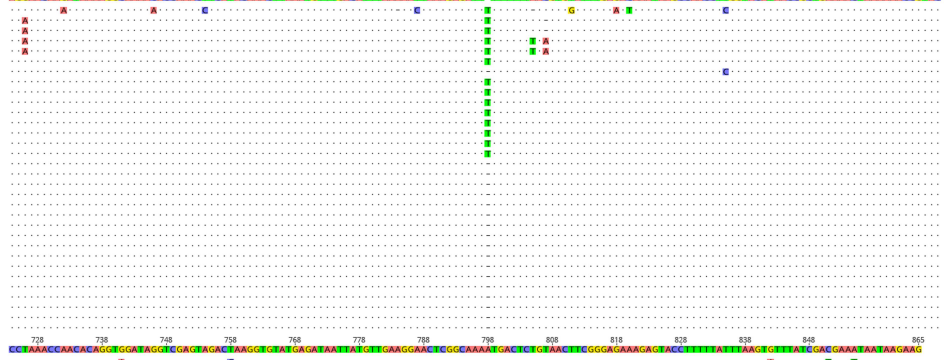
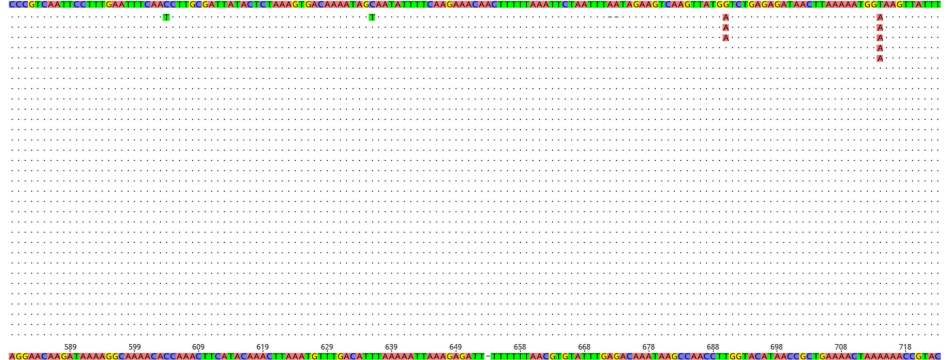
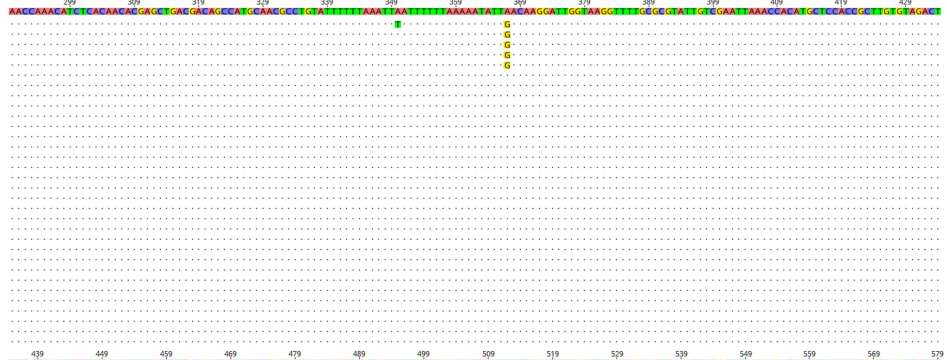
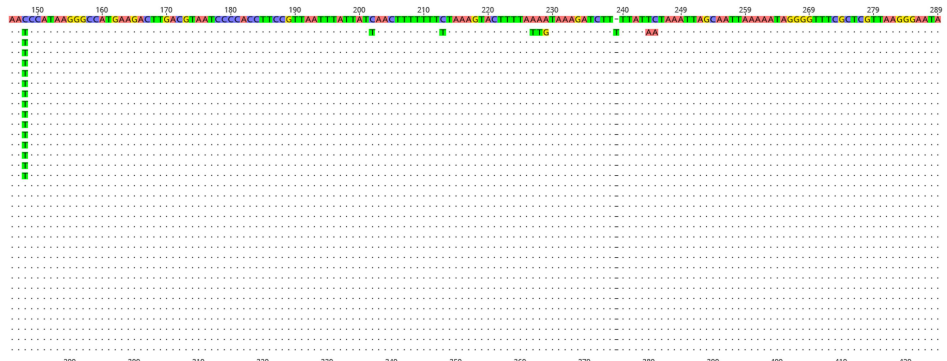
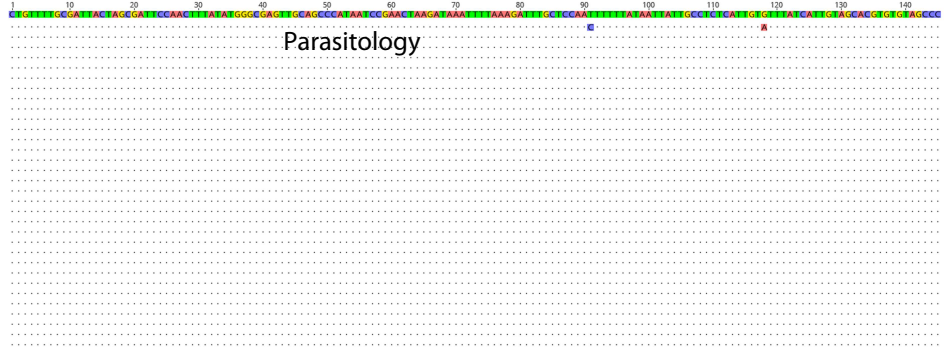
Consensus
 SAP817 *Aphanomyces frigidophilus*
 APO03
 Iwo0113
 SAP-Malaga5
 GiS5
 Kv1
 L10
 L1
 UEF_VEN5/14
 UEF_AT1D
 UEF_Oh1B
 Udon4
 UEF_T2B
 UEF_Oh1D
 UEF_Oi2E
 SIGM9
 AUT2_1
 UEF_T16K
 UEF_T16-R27P
 UEF_T16-R25A
 UEF_SATR2
 UEF_SATR1
 UEF_KY3-3
 UEF_8866-2
 UEF_8147-4
 UEF_8140-1
 UEF_7208
 UEF_7204-4
 UEF_7203
 SAP-Pamplona1
 EsviraK047/99
 Pl

Consensus
 SAP817 *Aphanomyces frigidophilus*
 APO03
 Iwo0113
 SAP-Malaga5
 GiS5
 Kv1
 L10
 L1
 UEF_VEN5/14
 UEF_AT1D
 UEF_Oh1B
 Udon4
 UEF_T2B
 UEF_Oh1D
 UEF_Oi2E
 SIGM9
 AUT2_1
 UEF_T16K
 UEF_T16-R27P
 UEF_T16-R25A
 UEF_SATR2
 UEF_SATR1
 UEF_KY3-3
 UEF_8866-2
 UEF_8147-4
 UEF_8140-1
 UEF_7208
 UEF_7204-4
 UEF_7203
 SAP-Pamplona1
 EsviraK047/99
 Pl

Consensus
 SAP817 *Aphanomyces frigidophilus*
 APO03
 Iwo0113
 SAP-Malaga5
 GiS5
 Kv1
 L10
 L1
 UEF_VEN5/14
 UEF_AT1D
 UEF_Oh1B
 Udon4
 UEF_T2B
 UEF_Oh1D
 UEF_Oi2E
 SIGM9
 AUT2_1
 UEF_T16K
 UEF_T16-R27P
 UEF_T16-R25A
 UEF_SATR2
 UEF_SATR1
 UEF_KY3-3
 UEF_8866-2
 UEF_8147-4
 UEF_8140-1
 UEF_7208
 UEF_7204-4
 UEF_7203
 SAP-Pamplona1
 EsviraK047/99
 Pl

Consensus
 SAP817 *Aphanomyces frigidophilus*
 APO03
 Iwo0113
 SAP-Malaga5
 GiS5
 Kv1
 L10
 L1
 UEF_VEN5/14
 UEF_AT1D
 UEF_Oh1B
 Udon4
 UEF_T2B
 UEF_Oh1D
 UEF_Oi2E
 SIGM9
 AUT2_1
 UEF_T16K
 UEF_T16-R27P
 UEF_T16-R25A
 UEF_SATR2
 UEF_SATR1
 UEF_KY3-3
 UEF_8866-2
 UEF_8147-4
 UEF_8140-1
 UEF_7208
 UEF_7204-4
 UEF_7203
 SAP-Pamplona1
 EsviraK047/99
 Pl

Consensus
 SAP817 *Aphanomyces frigidophilus*
 APO03
 Iwo0113
 SAP-Malaga5
 GiS5
 Kv1
 L10
 L1
 UEF_VEN5/14
 UEF_AT1D
 UEF_Oh1B
 Udon4
 UEF_T2B
 UEF_Oh1D
 UEF_Oi2E
 SIGM9
 AUT2_1
 UEF_T16K
 UEF_T16-R27P
 UEF_T16-R25A
 UEF_SATR2
 UEF_SATR1
 UEF_KY3-3
 UEF_8866-2
 UEF_8147-4
 UEF_8140-1
 UEF_7208
 UEF_7204-4
 UEF_7203
 SAP-Pamplona1
 EsviraK047/99
 Pl



Supplementary Table 1. Haplotypes found in *Aphanomyces astaci* sequences for the mitochondrial ribosomal rnnS and rnnL subunits. The first line shows the relative position of rnnS and rnnL subunits and the second line the SNPs found in the concatenated sequence (rnnS + rnnL) of 866 pb. Columns 2 and 3 refer to the SNP position in the 512 pb sequence analysed for the rnnS mtDNA subunit. Columns 4-11 refer to the SNP position in the 355 pb sequence analysed for the rnnL mtDNA subunit. Bold letters indicate the transitions and the transversions at each relative position.

Haplotype	148	367	546	570	582	652	661	663	691	841	849
a	T	A	G	T	G	T	A	C	T	G	C
b	C	A	G	T	G	-	A	C	T	G	C
d1	T	G	G	A	A	T	T	A	T	A	C
d2	T	G	A	A	A	-	T	A	T	A	C
e	T	A	G	T	G	-	A	C	C	G	A